Mechanics & Industry **20**, 206 (2019)

https://doi.org/10.1051/meca/2019023

Mechanics & Industry

Available online at:
www.mechanics-industry.org

Regular Article

Performance investigation of organic Rankine-vapor compression refrigeration integrated system activated by renewable energy

B. Saleh[1,2,*], Ayman A. Aly[1,2], Ageel F. Alogla[1], Awad M. Aljuaid[1], Mosleh M. Alharthi[3], Khaled I.E. Ahmed[2,4], and Y.S. Hamed[5,6]

[1] Mechanical Engineering Department, College of Engineering, Taif University, PO Box 888, Taif, Saudi Arabia
[2] Mechanical Engineering Department, Faculty of Engineering, Assiut University, PO Box 71516, Assiut, Egypt
[3] Electrical Engineering Department, College of Engineering, Taif University, PO Box 888, Taif, Saudi Arabia
[4] Mechanical Engineering Department, Faculty of Engineering, King Abdulaziz University, PO Box 21589, Jeddah, Saudi Arabia
[5] Physics and Engineering Mathematics Department, Faculty of Electronic Engineering, Menoufia University, PO Box 32952, Menouf, Egypt
[6] Mathematics and Statistics Department, Faculty of Science, Taif University, PO Box 888, Taif, Saudi Arabia

Received: 13 January 2018 / Accepted: 22 March 2019

Abstract. In this article, the performance and working fluid selection for an organic Rankine cycle-vapor compression refrigeration (ORC–VCR) integrated system activated by renewable energy is investigated. The performance of the system is described by the system coefficient of performance (COP_S), and the refrigerant mass flow rate per kilowatt refrigeration capacity ($\dot{m}_{total}$). Twenty-three pure substances are proposed as working fluids for the integrated system. The basic integrated system performance is assessed and compared using the proposed working fluids. The basic VCR cycle works between 35 and 0 °C, while the basic ORC works between 35 and 100 °C. The impacts of different operating parameters such as the evaporator, the boiler, and the condenser temperatures on the ORC–VCR system performance are also examined. The results show that the cyclopentane accomplished the highest system performance under all investigated operating conditions. Accordingly, among the examined 23 working fluids, cyclopentane is the most appropriate working fluid for the integrated system from the viewpoints of environmental concerns and system performance. Nevertheless, due to its high flammability, further restrictions should be taken. The basic integrated system COP_S, refrigeration effect, and the corresponding $\dot{m}_{total}$ utilizing cyclopentane are 0.654, 361.3 kW, and 0.596×10^{-2} kg/(s kW), respectively.

Keywords: Alternative working fluids / integrated system / organic Rankine cycle / vapor refrigeration cycle / renewable energy

1 Introduction

Low-grade thermal energy such as geothermal energy, solar energy, low-temperature waste heat from industrial plants, and exhaust gases from engines and turbines extensively exists in the world. Besides their renewable nature, they are also considered as free and clean energy sources since there is no additional direct carbon emission. Most of these heat sources cannot be used efficiently by the traditional power machines. In order to make better usage of low-temperature heat sources, researches on the combination of refrigeration and power systems have been conducted since the 1990s. Many systems arrangements have been suggested and inspected in the previous decade. These systems can transform low-grade heat to beneficial cooling or power energy. An organic Rankine cycle (ORC) driven by renewable energy and waste heat may be combined with vapor compression refrigeration (VCR) system for production of refrigeration or electricity [1,2].

The working fluids performance in an organic Rankine cycle-vapor compression refrigeration (ORC–VCR) integrated system is considerable. Numerous studies have been carried out to select the best fluid for the integrated system [3–7]. Saleh [4] suggested 10 substances as fluids for an ORC–VCR combined system. The results exhibited that R600 is the best fluid for the combined system. A parametric study and a regression analysis for a combined ORC and a cascade refrigeration system using natural refrigerants as working fluids were performed by Lizarte et al. [8]. The highest system coefficient of performance (COP_S) value was 0.79. The performance and working fluid

* e-mail: bahaa_saleh69@yahoo.com

selection for a VCR–ORC system were examined by Asim et al. [9]. Based on thermodynamics, R600a-R123 was chosen as the fluid pair for the integrated system. They concluded that the COP of the system was improved from 3.10 to 3.54 compared with that of the VCR cycle subsystem. Cihan [10] performed a theoretical analysis of a combined system with R600, R600a, R245fa, and pentane as working fluids. The results showed that R601 is the most appropriate fluid for the combined system. Li et al. [11] evaluated the performance of an ORC–VCR system using R1270, R600, R290, and R600a. The results indicated that butane is the best fluid for the system with COP_S of 0.47. Aphornratana and Sriveerakul [12] examined the performance of a combined system. With R134a, for a condenser temperature (T_{cond}) of 35 °C and an evaporator temperature (T_{eva}) of −10 °C, the COP_S was 0.125. Bu et al. [13,14] analyzed a combined system utilizing R245fa, R123, R600, R600a, R290, and R134a as working fluids. They concluded that R600a is the most appropriate fluid for the system. Han et al. [15] investigated experimentally an integrated power refrigeration system that utilizes an ammonia–water binary fluid. The COP_S was 0.47 with cooling output of 11.7 kW. Wang et al. [16] performed an experimental study and theoretical analysis for an ORC–VCR system. The system attained a COP_S value of approximately 0.5. Molés et al. [17] inspected an ORC–VCR system utilizing two working fluids for the ORC and two different fluids for the VCR. The results showed that the most suitable fluid for the power subsystem is R1336mzz(Z), while R1234ze(E) is the best fluid for the cooling subsystem. Nasir and Kim [18] examined the performance of seven working fluids, in an ORC–VCR system driven by low-grade thermal energy. They found that R600a is the most appropriate fluid for VCR cycle and R134a for ORC. Li et al. [19] performed energetic analysis for an ORC–VCR system using different working fluids. They concluded that R134a is the best fluid for the combined system. Kim and Perez-Blanco [20] performed a theoretical analysis for an ORC–VCR system using different working fluids. They concluded that R600 and R600a attained the highest system performance.

In this paper, the performance analysis of ORC–VCR integrated system for refrigeration or power production running with various working fluids is conducted. The inspected system is powered by a low-grade renewable heat source like waste heat or geothermal heat at around 115 °C. Twenty-three common and new pure hydrofluorocarbons (HFCs), hydrocarbons (HCs), fluorocarbons (FCs), hydrofluoroolefins (HFOs), and hydrofluoroethers (HFEs) are suggested and assessed as working fluids for the integrated system. The inspected substances are R161, RC318, butane (R600), pentane (R601), isobutane (R600a), isopentane (R601a), hexane (R602), R152a, perfluoropentane (C5F12), R236fa, R245ca, R236ea, R245fa, RE245cb2, isohexane (R602a), R1234ze(E), RE245fa2, RE170, RE347mcc, R365mfc, heptane (R603), octane (R604), and cyclopentane. The performance of the integrated system was assessed by the performance parameters, i.e., COP_S and the refrigerant total mass flow rate per kilowatt refrigeration capacity ($\dot{m}_{\mathrm{total}}$). The impacts of some operating parameters like the condenser, evaporator, and boiler temperatures on the system performance were also studied.

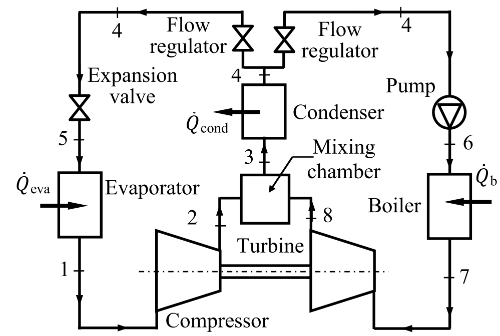

Fig. 1. Scheme of the proposed ORC–VCR integrated system.

2 The system description and selection of working fluid

Figure 1 illustrates a scheme of the inspected integrated system, which includes two subsystems: the ORC, specified as 3-4-6-7-8-3, and the VCR cycle, specified as 1-2-3-4-5-1. The ORC contains turbine, pump, evaporator, and condenser. The VCR cycle consists of a compressor, an evaporator, a condenser, and a throttle devise. The features of the proposed system are as follows: (a) use the same fluid for both subsystems, (b) the turbine output power is equal to the compressor power, and (c) the system uses one condenser for the two subsystems. Two flow regulators were utilized to regulate flexibly the mass flow rate of the working fluid to VCR and ORC subsystems.

The working fluid selection for the integrated system is very important. An ideal fluid must accomplish both maximum system performance and lowest environmental concerns. Hydrochlorofluorocarbons (HCFCs) and chlorofluorocarbons (CFCs) are ozone-depleting fluids. Therefore, FCs and HFCs are used as alternative fluids for combined systems, ORC, and VCR cycle because they have zero ozone depletion potential (ODP) [1,21]. FCs and HFCs have high global warming potential (GWP), accordingly their use are controlled. Therefore, researches are still ongoing for alternative fluids, which may have lesser environmental concerns. As one of the proposals, HCs are considered as alternative fluids. HCs are environmentally friendly, have superior thermophysical properties, and have very low GWP [22]. The HCs are highly soluble in mineral oils, environmentally friendly, and chemically stable, but they are flammable. However, with proper safety protections, flammability will not be considered the largest challenge against HCs. HFEs are low toxic, nonflammable, have very low GWP, short atmospheric lifetime (ALT), and zero ODP; accordingly, they have been suggested as working fluids for thermal systems [23]. Moreover, many HFOs were recommended as working fluids due to their low environmental impacts [1,17].

The outline of temperature–entropy (T–s) diagram is a necessary property for fluid categorization. The fluids are categorized as isentropic, dry, and wet. For wet fluids, condensation takes place during the expansion in the turbine. This might be a reason for turbine blade erosion. Conversely, in the case of isentropic and dry fluids, there is

Table 1. Properties of the inspected fluids.

Fluid	Physical properties					Environmental data			Safety data	
	M g/mol	NBP °C	T_{crit} °C	P_{crit} MPa	$v_{crit} \times 10^3$ m^3/kg	ALT year	ODP	GWP 100 year	LFL %	Safety group
R161	48.1	−37.6	102.1	5.010	3.31	0.18	0.0	12	3.8	–
R1234ze(E)	114.0	−19.0	109.4	3.635	2.04	0.045	0.0	<1	7.6	A2L
R152a	66.1	−24.0	113.3	4.517	2.72	1.10	0.0	133	4.8	A2
RC318	200.0	−5.98	115.2	2.778	1.61	320 0	0.0	10300	–	A1
R236fa	152.0	−1.50	124.9	3.200	1.81	242.0	0.0	9820	–	A1
RE170	46.1	−24.8	127.2	5.337	3.65	0.015	0.0	1	3.4	A3
RE245cb2	150.1	5.62	133.7	2.886	2.00	4.90	0.0	680	–	–
R600a	58.1	−11. 8	134.7	3.629	4.44	0.016	0.0	~20	1.6	A3
R236ea	152.0	6.17	139.3	3.420	1.77	11.0	0.0	1410	–	–
C5F12	288.0	29.8	147.4	2.045	1.64	4100	0.0	9160	–	–
R600	58.1	−0.49	152.0	3.796	4.39	0.018	0.0	~20	2.0	A3
R245fa	134.1	15.1	154.1	3.650	1.94	7.70	0.0	1050	–	B1
RE347mcc	200.1	34.2	164.6	2.476	1.91	5.0	0.0	553	none	A1
RE245fa2	150.1	29.3	171.7	3.433	1.94	5.5	0.0	659	–	–
R245ca	134.1	25.3	174.4	3.940	1.90	6.50	0.0	726	7.1	–
R365mfc	148.1	40.2	186.9	3.266	2.11	8.6	0.0	794	3.6	A3
R601a	72.2	27.8	187.2	3.378	4.24	12.0	0.0	4	1.32	A3
R601	72.2	36.1	196.6	3.370	4.31	12	0.0	4	1.4	A3
R602a	86.2	60.2	224.6	3.040	4.27	–	0.0	~20	1.2	A3
R602	86.2	68.7	234.7	3.034	4.29	–	0.0	~20	1.2	A3
Cyclopentane	70.1	49.3	238.6	4.571	3.73	0.007	0.0	<0.1	1.1	A3
R603	100.2	98.4	267.0	2.736	4.31	–	0.0	3	1.2	–
R604	114.2	125.6	296.2	296.17	4.26	–	0.0	3	1.0	–

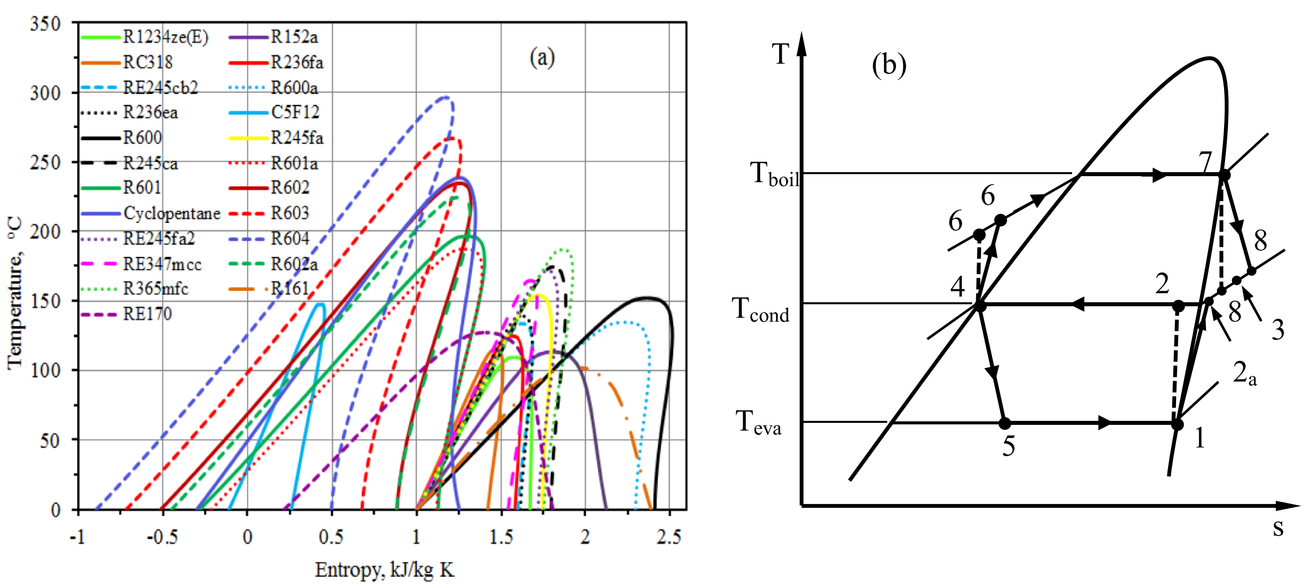

Fig. 2. (a) Inspected working fluids T–s diagrams. (b) T–s diagram of the integrated system.

no condensation. Consequently, in this paper all the assessed fluids are dry fluids except RE170, R161, and R152a, which are wet fluids. The thermodynamic properties and environmental and safety data of the inspected fluids are specified in Table 1 [24,25].

Figure 2a displays the T–s diagram of the inspected fluids; Figure 2b shows the T–s diagram of the integrated system. The processes in the system that are shown in Figure 2b can be described for each subsystem. The VCR cycle: Processes (1-2s and 1-2a) are isentropic and actual compression processes, process (8-2a-3) is an adiabatic mixing process, process (3-4) is a condensation process, process (4-5) is a throttling process, and process (5-1) is a vaporization process of the refrigerant through the evaporator. With respect to the ORC, processes ($4\text{-}6_S$ and $4\text{-}6_a$) are isentropic and actual pumping, process ($6_a\text{-}7$) is vaporization process of the working fluid across the boiler, and processes ($7\text{-}8_S$ and $7\text{-}8_a$) are isentropic and actual expansion in the turbine.

3 System energy analysis

The next assumptions are assumed to simplify the system modeling: (i) the system runs at a steady state, (ii) saturated states are supposed at the boiler, condenser, and evaporator exits, (iii) there is no heat loss in the pipelines, (iv) the pressure loss in the pipelines are neglected, and (v) flow losses, for example, the friction losses impacts and actual compression and expansion processes are taken into account by utilizing compressor, turbine, and pump efficiencies. The mathematical model of the integrated system displayed in Figure 1 is presented in the next sections.

Concerning the VCR cycle, the required power for the compressor, $\dot{W}_{\text{comp}}$, can be calculated as follows:

$$\dot{W}_{\text{comp}} = \dot{m}_{\text{VCR}}(h_1 - h_{2a}) = \frac{\dot{m}_{\text{VCR}}(h_1 - h_{2s})}{\eta_{\text{comp}}} \tag{1}$$

where $\dot{m}_{\text{VCR}}$ is the mass flow rate of the fluid in the VCR, h_1 is the specific enthalpy at the compressor entrance, h_{2s} and h_{2a} are the isentropic and actual specific enthalpies at the compressor outlet, respectively, and η_{comp} is the compressor isentropic efficiency.

The heat transfer rate to the refrigerant through the evaporator, $\dot{Q}_{\text{eva}}$, can be expressed as

$$\dot{Q}_{\text{eva}} = \dot{m}_{\text{VCR}}(h_1 - h_5) \tag{2}$$

where h_1 and h_5 are the specific enthalpies at the outlet and entrance of the evaporator, respectively, in kJ/kg.

The VCR cycle coefficient of performance, COP_{VCR}, is expressed as

$$\text{COP}_{\text{VCR}} = \frac{\dot{Q}_{\text{eva}}}{\dot{W}_{\text{comp}}} \tag{3}$$

Concerning the ORC, the power output from the turbine, $\dot{W}_{\text{turb}}$, is just sufficient to power the compressor:

$$\dot{W}_{\text{turb}} = \dot{W}_{\text{comp}} \tag{4}$$

The working fluid mass flow rate in the ORC, $\dot{m}_{\text{ORC}}$, can be expressed as

$$\dot{m}_{\text{ORC}} = \frac{\dot{W}_{\text{turb}}}{\eta_{\text{turb}} * (h_7 - h_{8s})} \tag{5}$$

where h_7 is specific enthalpy at the turbine entrance, h_{8s} is the isentropic specific enthalpy at the exit of the turbine, and η_{turb} is the turbine isentropic efficiency.

The rate of heat transfer in the boiler, $\dot{Q}_{\text{boil}}$, can be written as

$$\dot{Q}_{\text{boil}} = \dot{m}_{\text{ORC}}(h_7 - h_{6a}) \tag{6}$$

where h_{6a} is the actual specific enthalpy at the boiler inlet, and h_7 is the specific enthalpy at the boiler outlet.

The required power to the pump, $\dot{W}_{\text{pump}}$, can be expressed as

$$\dot{W}_{\text{pump}} = \dot{m}_{\text{ORC}}\,(h_{6a} - h_4) = \frac{\dot{m}_{\text{ORC}}(h_{6s} - h_4)}{\eta_{\text{pump}}} \tag{7}$$

where h_{6s} and h_{6a} are the isentropic and actual enthalpies at the pump outlet, respectively, h_4 is the enthalpy at the entrance of the pump, and η_{pump} is the efficiency of the pump.

The thermal efficiency of the ORC, η_{ORC}, is represented as

$$\eta_{\text{ORC}} = \frac{\dot{W}_{\text{turb}}}{\dot{Q}_{\text{boil}} + \dot{W}_{\text{pump}}} \tag{8}$$

The heat transfer rate from the fluid in the condenser, $\dot{Q}_{\text{cond}}$, can be expressed as

$$\dot{Q}_{\text{cond}} = (\dot{m}_{\text{ORC}} + \dot{m}_{\text{VCR}}) * (h_4 - h_3) \tag{9}$$

The COP_S of the integrated ORC–VCR system can be written as

$$\text{COP}_S = \eta_{\text{ORC}} \times \text{COP}_{\text{VCR}} = \frac{\dot{Q}_{\text{eva}}}{\dot{Q}_{\text{boil}} + \dot{W}_{\text{pump}}} \tag{10}$$

The working fluid total mass flow rate per kW cooling capacity, $\dot{m}_{\text{total}}$, in kg/(s·kW) is expressed as

$$\dot{m}_{\text{total}} = \frac{\dot{m}_{\text{ORC}} + \dot{m}_{\text{VCR}}}{\dot{Q}_{\text{eva}}} \tag{11}$$

A computer program is constructed to compute the performance of the integrated system using various fluids under different operating parameters and to examine the impacts of many working conditions on the performance of the system. The NIST REFPROP 9.1 database [26] was applied to get the properties of the investigated fluids. The basic values of the integrated system operating conditions and their ranges are specified in Table 2. The uppermost temperature of the boiler (T_{boil}) was kept constant at 100 °C, which is permitted to use renewable energy heat source at ~115 °C.

4 Results and discussion

The performance of an ORC–VCR integrated system activated by low-grade renewable energy source utilizing various fluids is assessed. The investigated fluids are R161, RC318, R600, R600a, R601a, R601, R602, perfluoropentane, R152a, R236fa, R1234ze(E), R245ca, R236ea, R245fa, RE245cb2, R602a, RE245fa2, RE170, RE347mcc, R365mfc, R603, R604, and cyclopentane. The critical temperatures of the inspected fluids exist between 102.1 °C for R161 and 296.17 °C for R604, as shown in Table 1.

A performance comparison of the basic integrated system utilizing all inspected fluids is presented in Table 3. Additionally, the T–s diagram type, cooling effect ($\dot{Q}_{eva}$), the power output from the turbine, and the actual quality at the turbine outlet (x_{8a}) are also specified in Table 3. The outcomes in Table 3 were gotten utilizing the basic values of the operating conditions as specified in Table 2. It is detected from the results in Table 3 that cyclopentane has the highest COP_S, $\dot{Q}_{eva}$, and the lowest $\dot{m}_{total}$ values. These values are 0.654, 361.3 kW, and 0.596×10^{-2} kg/(s · kW), respectively. Conversely, perfluoropentane with the uppermost molecular mass accomplishes the lower most COP_S, $\dot{Q}_{eva}$, values and the uppermost $\dot{m}_{total}$. These values are 0.43, 63.57 kW, and 3.2×10^{-2} kg/(s · kW), respectively. Accordingly, from the energetic analysis viewpoint, cyclopentane may be considered as a promising fluid for the integrated system.

The impacts of some selected working parameters such as T_{cond}, T_{eva}, and T_{boil} on the performance of the integrated system are explained in the next sections. In each subsection, the parameter whose impact is inspected varied within the range listed in Table 2 whereas the remaining operating conditions are kept constant and equal to the basic values presented in Table 2. The results show that all inspected operating conditions have similar impacts on the integrated system performance for all inspected fluids. Consequently, in the following figures, only some selected fluids from the 23 inspected fluids were drawn as examples.

Table 2. Operating conditions basic values.

Parameters	Basic values	Ranges
$\dot{m}_{VCR}$	1 kg/s	–
η_{pump}	0.8	–
η_{turb}	0.8	–
η_{comp}	0.75	–
T_{boil}	100 °C	60–100 °C
T_{cond}	35 °C	30–55 °C
T_{eva}	0 °C	−15–15 °C

Table 3. Basic ORC–VCR integrated system performance using all examined fluids.

Fluid	**Type**	$\dot{Q}_{eva}$, kW	$\dot{W}_{turb}$, kW	η_{ORC}, %	COP_{VCR}	COP_S	$\dot{m}_{total} \times 100$	x_{8a}
R161	Wet	300.3	60.64	11.61	4.95	0.575	0.951	0.77
R1234ze(E)	Dry	136.3	28.17	11.26	4.84	0.545	1.763	–
R152a	Wet	245.1	48.61	11.76	5.04	0.593	1.023	0.90
RC318	Dry	76.13	16.76	10.48	4.54	0.476	2.878	–
R236fa	Dry	115.7	23.90	11.16	4.84	0.540	1.930	–
RE170	Wet	350.8	68.93	11.99	5.09	0.610	0.676	0.96
RE245cb2	Dry	118.0	24.46	10.99	4.82	0.530	1.845	–
R600a	Dry	270.7	54.56	11.56	4.96	0.574	0.813	–
R236ea	Dry	124.6	25.41	11.24	4.91	0.551	1.751	–
C5F12	Dry	63.57	14.30	9.659	4.45	0.429	3.242	–
R600	Dry	301.1	59.59	11.67	5.05	0.589	0.720	–
R245fa	Dry	158.7	31.39	11.52	5.05	0.582	1.382	–
RE347mcc	Dry	104.9	21.84	10.65	4.80	0.512	2.005	–
RE245fa2	Dry	150.7	29.97	11.36	5.03	0.571	1.417	–
R245ca	Dry	170.3	33.52	11.55	5.08	0.587	1.269	–
R365mfc	Dry	158.5	31.42	11.33	5.05	0.572	1.330	–
R601a	Dry	285.3	56.00	11.51	5.10	0.586	0.739	–
R601	Dry	304.8	59.44	11.59	5.13	0.595	0.692	–
R602a	Dry	286.2	55.88	11.43	5.12	0.585	0.728	–
R602	Dry	303.7	58.93	11.56	5.16	0.596	0.687	–
Cyclopentane	Dry	361.3	67.71	12.25	5.34	0.654	0.596	–
R603	Dry	303.1	58.75	11.52	5.16	0.594	0.686	–
R604	Dry	302.5	58.60	11.51	5.163	0.594	0.685	–

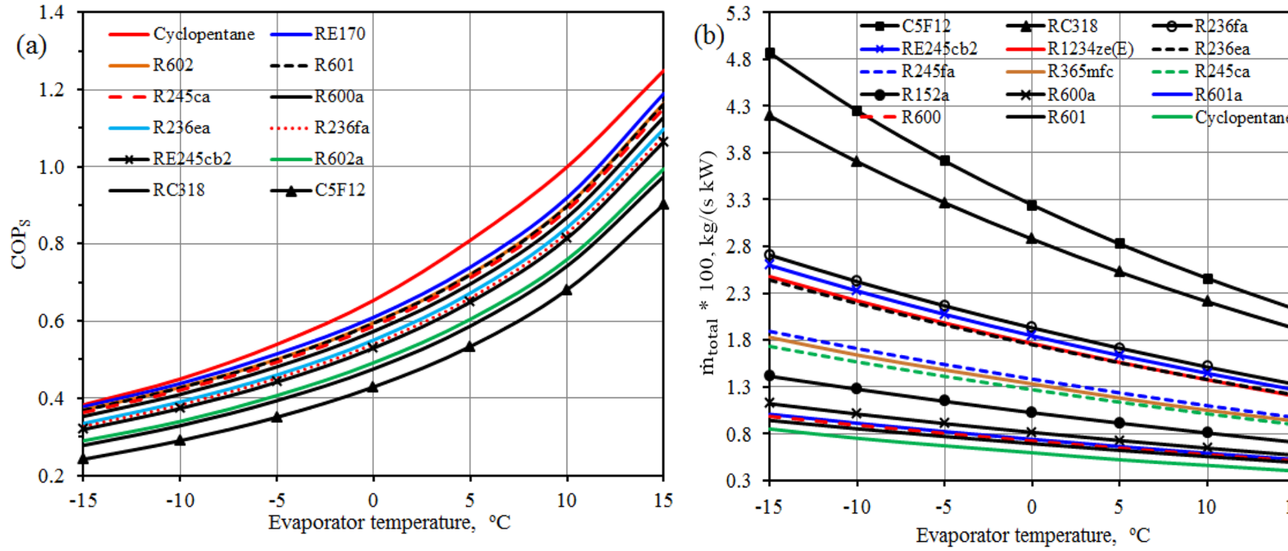

Fig. 3. Impact of T_{eva} on the COP_S (a) and $\dot{m}_{\text{total}}$ (b) using some inspected fluids in the basic system.

4.1 Evaporator temperature impact on the integrated system performance

The alterations of COP_S and $\dot{m}_{\text{total}}$ with T_{eva} using some selected investigated fluids in the basic integrated system are shown in Figure 3. As observed from Figure 3a, the COP_S increases with the increase of T_{eva} for all fluids. The alteration of T_{eva} has no impact on ORC. Thus, η_{ORC} is unchanged with the variation of T_{eva}. The evaporator saturation pressure increases with the increase of T_{eva} for all fluids. This leads to decline of $\dot{W}_{\text{comp}}$ with constant T_{cond}. Conversely, the increase of T_{eva} enhances the refrigeration effect. Both impacts enhance the COP_{VCR}. Based on equation (10), this results in improvement in the COP_S as T_{eva} increases. As T_{eva} varies from -15 up to 15 °C, the COP_S improves nearly 230% for all examined fluids.

The variations of $\dot{m}_{\text{total}}$ as function of the T_{eva} for the selected fluids in the basic system are exhibited in Figure 3b. As T_{eva} increases and with the assumption of fixed $\dot{m}_{\text{VCR}}$, the required $\dot{W}_{\text{comp}}$ declines. According to the assumption $\dot{W}_{\text{comp}} = \dot{W}_{\text{turb}}, \dot{W}_{\text{turb}}$ decreases as T_{eva} increases. The turbine-specific work is kept constant as T_{eva} changes. Based on equation (5), due to reducing $\dot{W}_t$ and fixed turbine-specific work, $\dot{m}_{\text{ORC}}$ must decline as T_{eva} rises. Therefore, $\dot{m}_{\text{total}}$ decreases as T_{eva} increases, as shown in Figure 3b. The alteration of $\dot{m}_{\text{total}}$ with T_{eva} is almost linear, as seen in Figure 3b. With the change of T_{eva} from -15 °C to 15 °C, the average decline of $\dot{m}_{\text{total}}$ is approximately 49% for all investigated fluids. Among the 23 investigated fluids, cyclopentane accomplishes the uppermost COP_S and the lowest $\dot{m}_{\text{total}}$ for all inspected T_{eva} values. Conversely, perfluoropentane attains the lowest COP_S and the highest $\dot{m}_{\text{total}}$ for all inspected T_{eva} values.

4.2 Boiler temperature impact on the integrated system performance

The influence of T_{boil} on the basic integrated system performance using some investigated fluids is shown in Figure 4. The COP_S alterations with the variations of T_{boil} are shown in Figure 4a. The COP_S enhances as T_{boil} improves. The enhancement in T_{boil} has no influence on the COP_{VCR} as $\dot{Q}_{\text{eva}}$ and $\dot{W}_{\text{comp}}$ are kept constant. The turbine-specific work rises as T_{boil} increases. Since it is assumed that $\dot{W}_{\text{comp}} = \dot{W}_{\text{turb}}$, and the truth that the $\dot{W}_{\text{comp}}$ is kept constant as T_{boil} increases, $\dot{m}_{\text{ORC}}$ should reduce as T_{boil} increases. The increase of T_{boil} results in enhancement of the specific heat added to the boiler. The trends of both $\dot{m}_{\text{ORC}}$ and boiler-specific heat with T_{boil} lead to decrease of $\dot{Q}_{\text{boil}}$ as T_{boil} increases. With the constant $\dot{W}_{\text{turb}}$, decline of $\dot{Q}_{\text{boil}}$, and the increase of T_{boil} and based on equation (8), η_{ORC} is enhanced. This results in the development of COP_S, as shown in Figure 4a. As seen from Figure 4a, the COP_S for all examined fluids at 100 °C T_{boil} are approximately double of those at 60 °C T_{boil}.

Figure 4b shows $\dot{m}_{\text{total}}$ as function of T_{boil} for some investigated fluids in the basic system. With the assumption that $\dot{m}_{\text{VCR}}$ is kept constant and $\dot{m}_{\text{ORC}}$ declines as T_{boil} increases, $\dot{m}_{\text{total}}$ reduces as T_{boil} increases, as shown in Figure 4b. Figure 4 also shows that among all inspected fluids, cyclopentane attains the uppermost COP_S and the lowermost $\dot{m}_{\text{total}}$ for all examined T_{boil}. Conversely, perfluoropentane accomplishes the lowest COP_S and the highest $\dot{m}_{\text{total}}$.

4.3 Condenser temperature impact on the integrated system performance

Figure 5 shows the T_{cond} impact on the performance of basic integrated system. Figure 5a shows the alteration of COP_S against T_{cond} for some examined fluids. As observed from Figure 5a, T_{cond} has a great impact on the COP_S. This is because of the impact of T_{cond} on the ORC and VCR subsystems. The rejected heat is constrained by T_{cond}, which is an additional restriction to improve the system efficiency in addition to T_{boil}. Huge values of total heat rejected are unwanted to achieve large efficiencies in the two subcycles. Both pressure and enthalpy at the exit of the

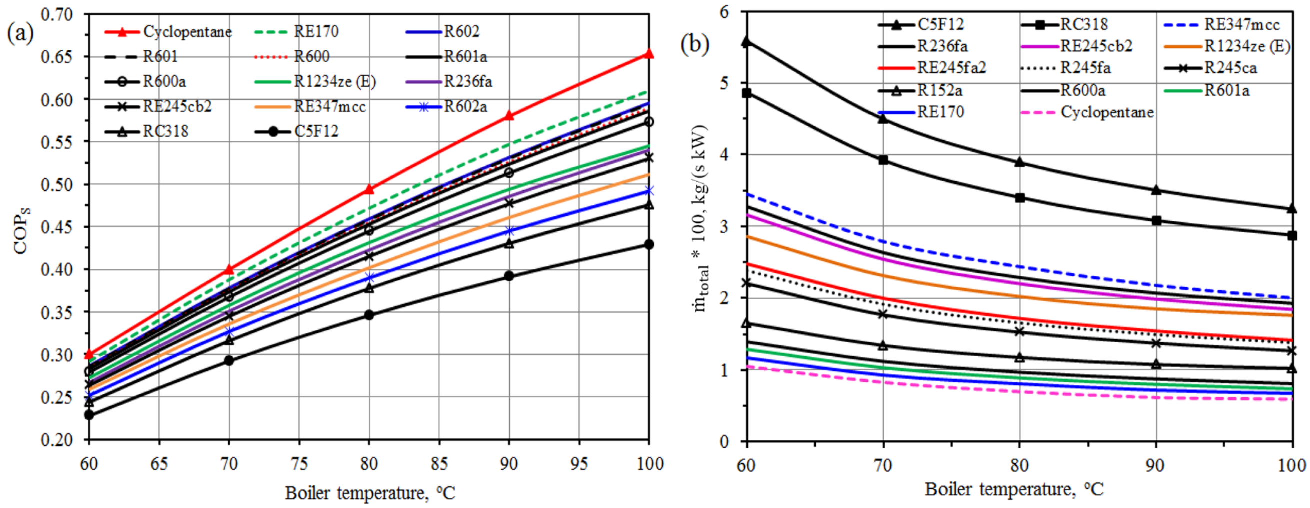

Fig. 4. Impact of T_{boil} on the COP_S (a) and $\dot{m}_{\text{total}}$ (b) using some investigated fluids in the basic system.

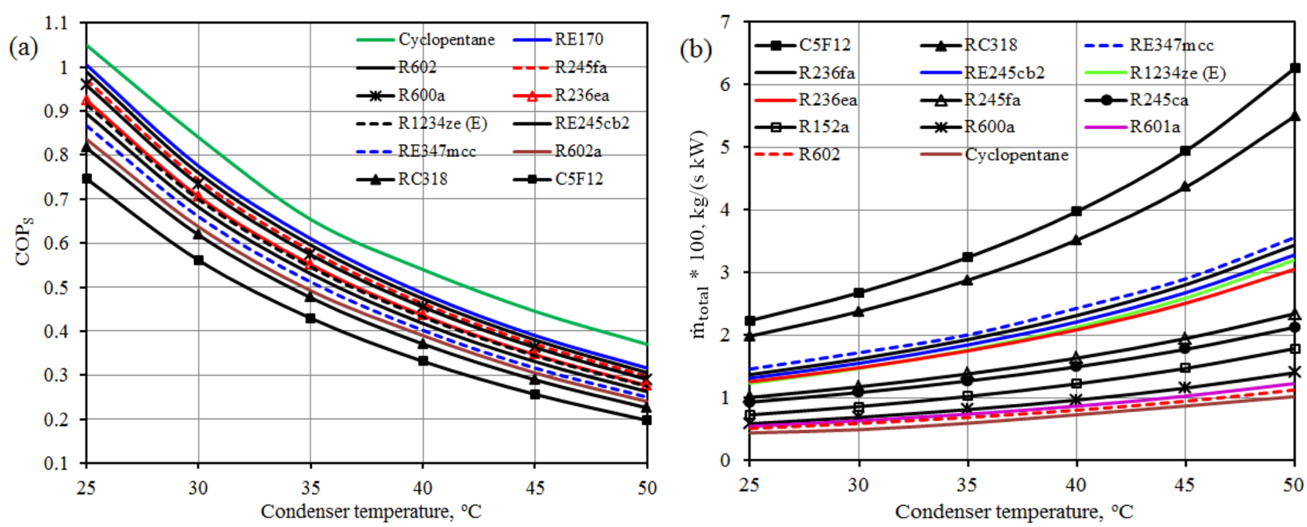

Fig. 5. Impact of T_{cond} on the COP_S (a) and $\dot{m}_{\text{total}}$ (b) using some investigated fluids in the basic system.

compressor increase with the enhancement of T_{cond} with constant temperature and pressure at the entrance of the compressor. This results in a decline of $\dot{Q}_{\text{eva}}$, increase of $\dot{W}_{\text{comp}}$, and decline of COP_{VCR}. Moreover, the increase of T_{cond} leads to increase of $\dot{W}_{\text{t}}$ because of the assumption of $\dot{W}_{\text{comp}} = \dot{W}_{\text{rurb}}$ and accordingly the $\dot{Q}_{\text{eva}}$increase of $\dot{m}_{\text{ORC}}$ to attain the assumption. The increase of $\dot{m}_{\text{ORC}}$ results in increase of $\dot{Q}_{\text{boil}}$. But the rate at which $\dot{Q}_{\text{boil}}$ increases is greater than that of $\dot{W}_t$, which results in the decline of η_{ORC}. Based on equation (10), the decrease of both COP_{VCR} and η_{ORC} results in decrease of COP_S. As noticed in Figure 5a, the COP_{S} declines as T_{cond} increases for all inspected fluids. As T_{cond} changes from 25 to 50 °C, COP_S declines by nearly 69% for all examined fluids. In comparison to all studied fluids, cyclopentane achieves the maximum thermal efficiency, while perfluoropentane attains the lowest thermal efficiency for all inspected T_{cond}. With T_{cond} equal to 35 °C and the basic values for the remaining operating conditions, COP_S utilizing cyclopentane is larger than that those of perfluoropentane by about 34.3%.

The change of $\dot{m}_{\text{total}}$ with T_{cond} for all inspected fluids in the basic integrated system is shown in Figure 5b. As T_{cond} increases, the required $\dot{W}_{\text{comp}}$ increases, and to achieve the assumption of $\dot{W}_{\text{comp}} = \dot{W}_{\text{rurb}}$ (Eq. (4)), the $\dot{m}_{\text{ORC}}$ should be increased. With the increase of $\dot{m}_{\text{ORC}}$ and with fixed $\dot{m}_{\text{VCR}}$, $\dot{m}_{\text{total}}$ increases as T_{cond} increases. The common tendency in Figure 5b is increase of $\dot{m}_{\text{total}}$ with the increase of T_{cond} for all inspected fluids. In comparison to all inspected fluids, the lowermost $\dot{m}_{\text{total}}$ was achieved by the bottommost molecular mass fluids. Conversely, the fluids with the uppermost molecular mass attained the highest $\dot{m}_{\text{total}}$ for all inspected T_{cond}. At T_{cond} equal to 50 and 25 °C, $\dot{m}_{\text{total}}$ values in the case of perfluoropentane are nearly 6.1 and 5.1 times those of cyclopentane, respectively. As T_{cond} changes from 25 to 50 °C using cyclopentane, $\dot{m}_{\mathrm{total}}$ increases by almost 132%.

To summarize, among all inspected fluids, cyclopentane achieves the highest COP_S and the lowest $\dot{m}_{\mathrm{total}}$ under all inspected working parameters. Conversely, perfluoropentane attains the lowest COP_S and the highest $\dot{m}_{\mathrm{total}}$ under all inspected working parameters. Therefore, cyclopentane may be considered the most convenient fluid for the integrated system. Cyclopentane is strongly flammable, which is the main challenge contrary to its usage. However, with additional safety cautions, the flammability will not be the problem in using cyclopentane.

5 Conclusions

The performance and working fluid selection for an ORC–VCR integrated system powered by renewable energy was studied. Numerous pure fluids, i.e., R161, RC318, R600, R601, R600a, R601a, R152a, R602, perfluoropentane, R245ca, R236fa, R245fa, R236ea, RE245cb2, R602a, R1234ze(E), RE245fa2, RE170, RE347mcc, R365mfc, R603, R604, and cyclopentane, were suggested as working fluids for the integrated system. The impacts of some operating conditions, i.e., the evaporator, condenser, and boiler temperatures, on the performance of the integrated system were also examined.

The results show that the highest thermal efficiency and the lowest mass flow rate were achieved by cyclopentane. Among the 23 inspected fluids, cyclopentane is the best working fluid for the integrated system to recapture low-grade renewable energy with a temperature between 75 and 115 °C. Since cyclopentane is highly flammable, supplementary precautions must be taken. The subsequent results were acquired using cyclopentane as working fluid. The COP_S and $\dot{m}_{\mathrm{total}}$ values at 100 °C boiler temperature equal 2.18 and 0.57 times, respectively, those at boiler temperature of 60 °C. The COP_S and $\dot{m}_{\mathrm{total}}$ values at 25 °C condenser temperature equal 2.84 and 0.43 times, respectively, those at condenser temperature of 50 °C. The COP_S and $\dot{m}_{\mathrm{total}}$ values at 15 °C evaporator temperature equal 3.26 and 0.47 times those at evaporator temperature of −15 °C, respectively. When the condenser temperature equals 25 °C and the remaining parameters at their basic values, the highest COP_S and the corresponding $\dot{m}_{\mathrm{total}}$ are 1.05 and 0.44×10^{-2} kg/(s · kW), respectively.

Acknowledgments. This study is supported by Taif University under research grant 1-439-6067. The authors would like to thank Taif University for financial support.

References

[1] W. Sun, X. Yue, Y. Wang, Exergy efficiency analysis of ORC (organic Rankine cycle) and ORC based combined cycles driven by low-temperature waste heat, Energy Convers. Manage. 135 (2017) 63–73

[2] B. Saleh, Energy and exergy analysis of an integrated organic Rankine cycle-vapor compression refrigeration system, Appl. Therm. Eng. 141 (2018) 697–710

[3] C. Yue, F. You, Y. Huang, Thermal and economic analysis of an energy system of an ORC coupled with vehicle air conditioning, Int. J. Refrig. 64 (2016) 152–167

[4] B. Saleh, Parametric and working fluid analysis of a combined organic Rankine-vapor compression refrigeration system activated by low-grade thermal energy, J. Adv. Res. 7 (2016) 651–660

[5] H. Chang, Z. Wan, Y. Zheng, X. Chen, S. Shu, Z. Tu, S.H. Chan, Energy analysis of a hybrid PEMFC-solar energy residential micro CCHP system combined with an organic Rankine cycle and vapor compression cycle, Energy Convers. Manage. 142 (2017) 374–384

[6] K. Braimakis, A. Thimo, S. Karellas, Technoeconomic analysis and comparison of a solar-based biomass ORC-VCC system and a PV heat pump for domestic trigeneration, J. Energy Eng. 143 (2017) 04016048

[7] D. Wu, L. Aye, T. Ngo, P. Mendis, Optimisation and financial analysis of an organic Rankine cycle cooling system driven by facade integrated solar collectors, Appl. Energy 185 (2017) 172–182

[8] R. Lizarte, M.E. Palacios-Lorenzo, J.D. Marcos, Parametric study of a novel organic Rankine cycle combined with a cascade refrigeration cycle (ORC-CRS) using natural refrigerants, Appl. Therm. Eng. 127 (2017) 378–389

[9] M. Asim, M.K.H. Leung, Z. Shan, Y. Li, D.Y.C. Leung, M. Ni, Thermodynamic and thermo-economic analysis of integrated organic Rankine cycle for waste heat recovery from vapor compression refrigeration cycle, Energy Procedia 143 (2017) 192–198

[10] E. Cihan, Cooling performance investigation of a system with an organic Rankine cycle using waste heat sources, J. Therm. Sci. Technol. 34 (2014) 101–109

[11] H. Li, X. Bu, L. Wang, Z. Long, Y. Lian, Hydrocarbon working fluids for a Rankine cycle powered vapor compression refrigeration system using low-grade thermal energy, Energy Build. 65 (2013) 167–172

[12] S. Aphornratana, T. Sriveerakul, Analysis of a combined Rankine-vapour compression refrigeration cycle, Energy Convers. Manage. 51 (2010) 2557–2564

[13] X. Bu, L. Wang, H. Li, Performance analysis and working fluid selection for geothermal energy-powered organic Rankine-vapor compression air conditioning, Geothermal Energy 1–2 (2013) 1–14

[14] X. Bu, L. Wang, H. Li, Working fluids selection for fishing boats waste heat powered organic Rankine-vapor compression ice maker, Heat Mass Transf. 50 (2014) 1479–1485

[15] W. Han, Q. Chen, L. Sun, S. Mac, T. Zhao, D. Zheng, H. Jin, Experimental studies on a combined refrigeration/power generation system activated by low-grade heat, Energy 74 (2014) 59–66

[16] H. Wang, R. Peterson, K. Harada, E. Miller, R. Ingram-Goble, L. Fisher, Performance of a combined organic Rankine cycle and vapor compression cycle for heat activated cooling, Energy 36 (2011) 447–458

[17] F. Molés, J. Navarro-Esbrí, B. Peris, A. Mota-Babiloni, K. Kontomaris, Thermodynamic analysis of a combined organic Rankine cycle and vapor compression cycle system activated with low temperature heat sources using low GWP fluids, Appl. Therm. Eng. 87 (2015) 444–453

[18] M.T. Nasir, K.C. Kim, Working fluids selection and parametric optimization of an organic Rankine cycle coupled vapor compression cycle (ORC-VCC) for air conditioning using low grade heat, Energy Build. 129 (2016) 378–395

[19] Y.R. Li, X.Q. Wang, X.P. Li, J.N. Wang, Performance analysis of a novel power/refrigerating combined-system driven by the low-grade waste heat using different refrigerants, Energy 73 (2014) 543–553

[20] K.H. Kim, H. Perez-Blanco, Performance analysis of a combined organic Rankine cycle and vapor compression cycle for power and refrigeration cogeneration, Appl. Therm. Eng. 91 (2015) 964–974

[21] B. Saleh, Performance analysis and working fluid selection for ejector refrigeration cycle, Appl. Therm. Eng. 107 (2016) 114–124

[22] A.H. Antunes, E.P. Filho, Experimental investigation on the performance and global environmental impact of a refrigeration system retrofitted with alternative refrigerants, Int. J. Refrig. 70 (2016) 119–127

[23] E.K. Goharshadi, F. Moosavi, Prediction of thermodynamic properties of some hydrofluoroether refrigerants using a new equation of state, Fluid Phase Equilib. 238 (2005) 112–119

[24] J.M. Calm, G.C. Hourahan, Physical, safety, and environmental data summary for current and alternative refrigerants, in: Proceedings of the 23rd International Congress of Refrigeration, Prague, Czech Republic, ID: 915, 2011, pp. 1–22

[25] J.M. Calm, ARTI Refrigerant Database: Data Summaries – Volume 1: Single-Compound Refrigerants, Air-Conditioning and Refrigeration Technology Institute, Arlington, VA, 1999

[26] E.W. Lemmon, M.L. Huber, M.O. McLinden, Reference Fluid Thermodynamic and Transport Properties (REFPROP): Version 9.1, National Institute of Standards and Technology (NIST), Boulder, CO, 2013

Cite this article as: B. Saleh, A.A. Aly, A.F. Alogla, A.M. Aljuaid, M.M. Alharthi, K.I.E. Ahmed, Y.S. Hamed, Performance investigation of organic Rankine-vapor compression refrigeration integrated system activated by renewable energy, Mechanics & Industry **20**, 206 (2019)